

Adlayer inhomogeneity without lateral interactions: Rationalizing correlation effects in CO oxidation at RuO₂(110) with first-principles kinetic Monte Carlo

Sebastian Matera,^{1,a)} Hakim Meskine,¹ and Karsten Reuter^{1,2}

¹Fritz-Haber-Institut der Max-Planck-Gesellschaft, Faradayweg 4-6, D-14195 Berlin, Germany

²Department Chemie, Technische Universität München, Lichtenbergstr. 4, D-85747 Garching, Germany

(Received 1 November 2010; accepted 18 January 2011; published online 14 February 2011)

Microkinetic modeling of surface chemical reactions still relies heavily on the mean-field based rate equation approach. This approach is expected to be most accurate for systems without appreciable lateral interactions among the adsorbed chemicals, and there in particular for the uniform adlayers resulting in poisoned regimes with predominant coverage of one species. Using first-principles kinetic Monte Carlo simulations and the CO oxidation at RuO₂(110) as a showcase, we demonstrate that even in this limit mean-field rate equations fail to predict the catalytic activity by orders of magnitude. This deficiency is traced back to the inability to account for the vacancy pair formation that is kinetically driven by the ongoing reactions. © 2011 American Institute of Physics. [doi:10.1063/1.3553258]

I. INTRODUCTION

Microkinetic descriptions in heterogeneous catalysis account for the concerted interplay of all elementary processes in the catalytic cycle.¹ For a given reaction mechanism, i.e., ensemble of elementary steps and their individual rate constants, microkinetic modeling yields important information like the catalytic activity or the surface composition as a function of the surrounding gas-phase conditions. Within the realm of site-specific adsorption into an arrangement of active sites at the catalyst surface this requires, in principle, solving for a high-dimensional master equation.² In prevalent phenomenological microkinetics (PK), this is much simplified by the assumption of negligible correlations between species at different active sites. Under this mean-field approximation the master equation separates into a set of ordinary rate equations that only consider the average occupations at the surface. In contrast, modern kinetic Monte Carlo (kMC) simulations explicitly solve the master equation and thereby fully account for the detailed spatial distribution of the chemicals at the surface.³

Despite numerous reports on its deficiencies, the PK approach still represents the state-of-the-art in applied research. The general textbook reason cited for failures are significant lateral interactions among the adsorbed species.⁴ The resulting thermodynamic driving force for segregation leads to inhomogeneities in the adlayer that cannot be captured in a mean-field picture. On the other hand, in the absence of such lateral interactions and, in particular, at low coverages one would expect the approach to work quite reliably. At first glance, this should similarly hold for dense, but uniform adlayers that result in systems without lateral interactions in poisoned regimes. In such a regime, one species almost exclusively dominates the surface population, and for the few dilute

other species or vacancies in the adlayer the same reasoning as for the low coverage regime should apply. In this respect the results of a recent study⁵ that systematically compared PK with first-principles kMC simulations for the established microkinetic model of CO oxidation at RuO₂(110) (Ref. 6) were rather surprising. In this model there are no lateral interactions and PK was shown to deviate by orders of magnitude from the kMC data—in particular in the O-poisoned regime where the surface is characterized by a homogeneous O adlayer.

Here we analyze this failure in detail and trace it back to the inability of the mean-field PK approach in accounting for the tendency to form vacancy pairs in the adlayer. This tendency arises out of the ongoing reaction kinetics, i.e., the inhomogeneity is this time not thermodynamically but kinetically driven. This example underscores the danger of using the PK approach in practical work—even in a regime that one would believe to be one of the “save havens” in terms of the validity of the mean-field approximation.

II. THEORY

In chemical kinetics the rare event dynamics typical for surface catalytic processes is exploited by considering a time evolution that is coarse-grained to the discrete elementary steps of the reaction mechanism. For an arrangement of N active sites at the surface the state of the system in this coarse-grained description is at any given time t defined by the state vector $\mathbf{x} = (x_1, x_2, \dots, x_N)$, where x_i denotes the current occupation of site i . In the present example of CO oxidation $x_i = 0$, CO or empty. Assuming that in the time between the rare events the system loses all memory of the past, the system dynamics then obeys a simple Markovian master equation,³

$$\frac{\partial}{\partial t} P(\mathbf{x}, t) = \sum_{\mathbf{y}} W(\mathbf{x}|\mathbf{y})P(\mathbf{y}, t) - \sum_{\mathbf{y}} W(\mathbf{y}|\mathbf{x})P(\mathbf{x}, t), \quad (1)$$

^{a)}Electronic mail: matera@fhi-berlin.mpg.de.

where $P(\mathbf{x}, t)$ is the probability that the system is in state \mathbf{x} at time t , and $W(\mathbf{y}|\mathbf{x})$ is the transition probability (in units of frequency) to go from state \mathbf{x} to state \mathbf{y} .

In the established microkinetic model for the CO oxidation at RuO₂(110) (Ref. 6), that we consider here, there are no lateral interactions between different sites at the surface, and the individual elementary steps change either only the occupation of one site i or of two (neighboring) active sites i and j . In addition, the sites i and j are not all different, but are of certain site types a, b of the regular lattice of active sites offered by the solid surface. In this case the probabilities to move from one state to another take the form

$$W(\mathbf{x}|\mathbf{y}) = \sum_a \sum_{i \in a} k_a(x_i|y_i) \prod_{l \neq i} \delta_{x_l, y_l} + \sum_{a \geq b} \sum_{\langle ij \rangle, i \in a, j \in b} k_{ab}(x_i, x_j|y_i, y_j) \prod_{l \neq i, j} \delta_{x_l, y_l}, \quad (2)$$

where $\langle ij \rangle$ means nearest neighbors pairs. The probabilities thus do not depend on the occupations of the sites not directly involved in the reaction step. In particular, in Eq. (2) the first sum contains all one-site processes, such as the unimolecular adsorption and desorption of CO, while the second sum contains all two-site processes, such as the dissociative adsorption (associative desorption) of O₂, diffusion of O and CO, as well as the CO oxidation reactions modeled as associative CO₂ desorption. As illustrated in Fig. 1, the model considers two types of active site types ($a, b = \text{br}$ and cus) arranged in a rectangular lattice. The equivalence of all br and all cus sites in this lattice dramatically reduces the number of inequivalent rate constants to $k_a(A|B)$ and $k_{ab}(A, B|C, D)$, where A, B, C, D denote either O, CO, or a vacancy involved in the process. While the system can thus propagate between zillions of different system states \mathbf{x} , the total number of different rate constants that is needed to evolve the equation is very limited. In the CO oxidation model for RuO₂(110) this number is 26, and all of these rate constants were computed from first-principles using density-functional and harmonic transition state theory. With Ref. 6 providing a detailed account of these calculations, Table I summarizes these 26 elementary processes and the specific values for their rate constants under the gas-phase conditions considered below.

Kinetic Monte Carlo simulations achieve an explicit numerical solution of the thus defined master equation and

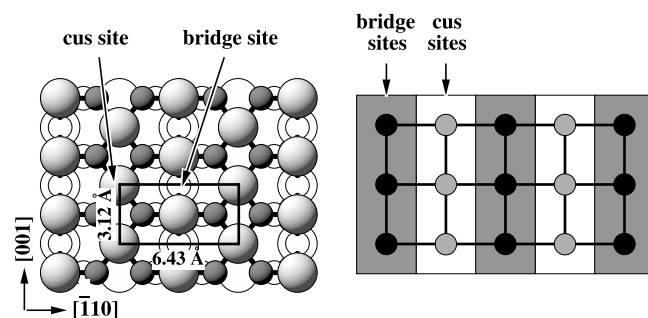


FIG. 1. (Left) panel: Top view of the RuO₂(110) surface showing the two prominent adsorption sites (br and cus). When focusing on these two sites, the surface can be coarse-grained to the lattice model shown schematically in the right panel, composed of alternating rows of br and cus sites.

TABLE I. Elementary reaction steps considered in the model together with their barriers and corresponding rate constants that result at the reaction conditions shown in Fig. 2 ($T = 600$ K, $p_{\text{O}_2} = 1$ atm, and varying p_{CO}). See Ref. 6 for details.

Process	ΔE (eV)	k (s ⁻¹)
Adsorption		
CO \rightarrow CO _{cus}	0	10 ⁴ –10 ¹⁰
CO \rightarrow CO _{br}	0	10 ⁴ –10 ¹⁰
O ₂ \rightarrow O _{cus} + O _{cus}	0	9.7 \times 10 ⁷
O ₂ \rightarrow O _{br} + O _{br}	0	9.7 \times 10 ⁷
O ₂ \rightarrow O _{br} + O _{cus}	0	9.7 \times 10 ⁷
Desorption		
CO _{cus} \rightarrow CO	1.60	9.2 \times 10 ⁶
CO _{br} \rightarrow CO	1.30	2.8 \times 10 ⁴
O _{cus} + O _{cus} \rightarrow O ₂	2.00	2.8 \times 10 ¹
O _{br} + O _{br} \rightarrow O ₂	4.60	4.1 \times 10 ⁻²¹
O _{br} + O _{cus} \rightarrow O ₂	3.30	3.4 \times 10 ⁻¹⁰
Diffusion		
CO _{cus} \rightarrow CO _{cus}	1.70	6.6 \times 10 ⁻²
CO _{br} \rightarrow CO _{br}	0.60	1.1 \times 10 ⁸
CO _{cus} \rightarrow CO _{br}	1.30	1.5 \times 10 ²
CO _{br} \rightarrow CO _{cus}	1.60	0.5
O _{cus} \rightarrow O _{cus}	1.60	0.5
O _{br} \rightarrow O _{br}	0.70	1.6 \times 10 ⁷
O _{cus} \rightarrow O _{br}	1.00	4.9 \times 10 ⁴
O _{br} \rightarrow O _{cus}	2.30	6.0 \times 10 ⁻⁷
CO ₂ formation		
CO _{cus} + O _{cus} \rightarrow CO ₂	0.9	1.7 \times 10 ⁵
CO _{br} + O _{br} \rightarrow CO ₂	1.5	1.6
CO _{cus} + O _{br} \rightarrow CO ₂	1.20	5.2 \times 10 ²
O _{cus} + CO _{br} \rightarrow CO ₂	0.80	1.2 \times 10 ⁶

therewith fully account for the detailed spatial distributions at the surface. In contrast, PK achieves a significant simplification of the problem by considering only the occupation probabilities at the different site types, i.e., the averaged coverage of site type a with species A ,

$$\theta_a(A, t) = \frac{1}{N_a} \sum_{i \in a} P_i(A, t) = \frac{1}{N_a} \sum_{i \in a} \sum_{\mathbf{x}} \delta_{x_i, A} P(\mathbf{x}, t), \quad (3)$$

where N_a is the number of sites of type a on the surface. $P_i(A, t)$ is the probability to find species A on site i , which is identical for all sites of the same type a for the homogeneous surface problem considered here. Using Eq. (1), one arrives at the equations governing the evolution of these different coverages

$$\begin{aligned} \frac{\partial}{\partial t} \theta_a(A, t) = & \sum_B k_a(A|B) \theta_B(A, t) - \sum_B k_a(B|A) \theta_a(A, t) \\ & + \sum_{bBCD} N_b^a k_{ab}(A, B|C, D) P_{ab}(C, D, t) \\ & - \sum_{bBCD} N_b^a k_{ab}(C, D|A, B) P_{ab}(A, B, t). \end{aligned} \quad (4)$$

Here, N_b^a is the number of nearest neighbor sites of type b around an a -site, i.e., a geometric factor prescribed by the underlying lattice structure. $P_{ab}(A, B, t)$ is the pair probability of finding species A at site type a and species B at a

neighboring site of type b at time t . In order to close these equations, PK makes a mean-field approximation and assumes that the probability of finding a species A in any site is completely independent of the occupation of any of the neighboring sites. In this absence of correlations between different sites the pair probabilities separate into simple products

$$P_{ab}(A, B, t) = \theta_a(A, t)\theta_b(B, t). \quad (5)$$

Inserting this expression into Eq. (4) leads finally to well-known rate equation expressions governing the individual surface coverages. For the CO oxidation at RuO₂(110) model these equations have been described in detail before.⁵

In empirical work the PK equations are often directly written down for a given reaction network.⁴ As the rate constant for any individual elementary step is then only a phenomenological quantity, it is often combined with the (in general equally unknown) geometric lattice factor N_b^a into one free fit parameter. In the quantitative comparison between kMC and PK aspired here, this cannot be done. For each elementary step the first-principles rate constant considered is exactly the same in kMC and PK, and in addition the lattice factor N_b^a needs to be explicitly considered in the PK expressions. For the rectangular RuO₂(110) rutile lattice with its alternating rows of br and cus sites, cf. Fig. 1, $N_b^a = 2$ for both site types.

Any observable difference between the kMC and PK simulations arises then solely from the mean-field approximation underlying PK. For these simulations we employ on the side of kMC exactly the same setup as described before, which is primarily characterized by a periodic boundary simulation cell comprising 200 br and 200 cus sites.⁵ In turn, the PK equations are integrated with the LSODE solver,⁷ employing a stiff backward differentiation discretization with a tolerance of 10^{-12} for the relative and absolute error in all six coverages. For both approaches these settings ensure only negligible numerical errors in the target quantities. Once steady-state has been reached, these target quantities are the individual coverages at the two active sites and the catalytic activity, measured as TOF in units of total number of product molecules per area and time.

III. RESULTS

As in the preceding work,⁵ we focus on a set of gas-phase conditions, representative for *in situ* experiments. These conditions are defined by a fixed O₂ pressure of $p_{O_2} = 1$ atm, fixed temperature $T = 600$ K, and varying CO pressure, 10^{-4} atm $< p_{CO} < 10^2$ atm. As such these conditions allow to discuss the three characteristic regimes of CO oxidation found in this model: at the lowest CO pressures considered the O-poisoned regime, i.e., a surface almost fully covered with O; at the highest CO pressures considered the CO-poisoned regime, i.e., a surface almost fully CO covered; and at pressures in between the catalytically most active state in which both intermediates are present at the surface in appreciable amounts. For this set of gas-phase conditions, Fig. 2 summarizes the central result obtained in our preceding work, namely, a striking difference between the TOFs simulated with PK and kMC. This difference extends primarily over the

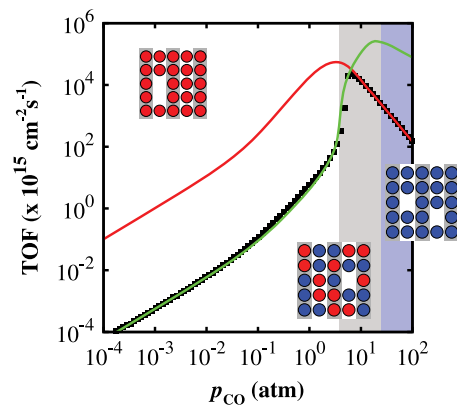


FIG. 2. Turn-over frequency (TOF) at $T = 600$ K, $p_{O_2} = 1$ atm, and varying p_{CO} obtained with kinetic Monte Carlo (kMC, black squares), phenomenological rate equations involving the mean-field approximation (PK, red line) and phenomenological rate equations corrected for vacancy pair correlation (PKmod, green line), see text. The insets show representative top views of the surface population in the three characteristic regimes that are additionally indicated by the different background shadings: Fully O-covered in the O-poisoned regime at low p_{CO} , fully CO-covered in the CO-poisoned regime at high p_{CO} , and coexistence of both species in the intermediate pressure regime.

O-poisoned regime, where PK fails to reproduce the kMC activity by several orders of magnitude. This deficiency is particularly striking as the surface is in this regime essentially characterized by a uniform O adlayer with an almost full coverage of both br and cus sites, cf. inset in Fig. 2. In the absence of lateral interactions in the model, one would expect a mean-field averaging to work very well, as e.g., found in the CO-poisoned regime where the quantitative agreement between kMC and PK shows that PK perfectly describes the corresponding uniform CO adlayer with almost full coverage of both br and cus sites.

Aiming to understand the reason for this curious discrepancy we start our analysis by realizing that the PK deficiency must result from an inadequate description of the rate-determining steps in the O-poisoned regime. This does not mean that the terms in Eq. (4) for the other steps in the reaction network are necessarily all well approximated in mean-field. However, any error in these terms will have hardly any impact on the overall reactivity. Using the degree of rate control approach we have recently shown that in the considered regime only five reactions are rate determining.⁸ These are the adsorption and desorption of CO at cus sites, adsorption and desorption of oxygen involving two cus sites, and the formation of CO₂ from O and CO adsorbed at neighboring cus sites. Since the adsorption and desorption of CO is a single-site process, it cannot be the reason for the discrepancy. In the absence of lateral interactions in the present model the terms associated with such processes are exactly described at the PK level without the need for a mean-field approximation, cf. Eq. (4). Oxygen desorption can equally be ruled out. For this process we need the pair probability to find an O_{cus} atom and a second one on the neighboring cus site, $P_{cus,cus}(O, O, t)$. At an essentially fully O-covered surface this probability is $P_{cus,cus}(O, O) \approx 1$. However, this also holds for the coverages, $\theta_{cus}(O, t) \approx 1$, and therewith for their product, $\theta_{cus}(O, t)\theta_{cus}(O, t) \approx 1$.

This leaves only the adsorption of O_2 into a cus vacancy pair and the reaction of a neighboring $O_{cus}-CO_{cus}$ pair as remaining rate-determining steps, i.e., the source of error must lie in the mean-field approximation for the pair probabilities $P_{cus,cus}(*, *)$ and/or $P_{cus,cus}(CO, O)$. For the former this approximation assumes no correlation between the two cus vacancies, i.e., the probability to find two vacancies next to each other is exactly the same as finding two vacancies at any other more distant site pair. In reality, cus vacancies at the fully O-covered surface are, however, almost exclusively created by either a $O_{cus}-O_{cus}$ desorption process or a $CO_{cus}-O_{cus}$ reaction process. Due to the much higher binding energy of oxygen at br sites equivalent desorption or reaction processes involving br site species occur with a probability that is orders of magnitude lower.⁶ Vacancies at cus sites are thus predominantly created as neighboring pairs in the uniform adlayer, cf. Fig. 2. Due to the relatively high diffusion barrier of 1.6 eV for O atoms along cus rows⁶ this correlation is furthermore not quickly erased with time. Instead the once created vacancy pair remains relatively immobile and bound together. Such a concerted appearance of vacancies next to each other cannot be grasped within a mean-field picture. If we find a vacancy on a cus site, one of the neighboring cus sites will also be empty in almost all cases, not with a probability proportional to the (very low) coverage of vacancies as mean-field implies. The required pair probability is therefore rather

$$P_{cus,cus}(*, *, t) \approx \frac{\theta_{cus}(*, t)}{2}, \quad (6)$$

i.e., at any given moment in time essentially all vacancies are grouped in pairs, such that the number of vacancy pairs are approximately half the number of vacancies in the adlayer.

This preferential existence of cus vacancy pairs also has bearings on the description of the $CO_{cus}-O_{cus}$ reaction. If a CO molecule adsorbs into one of the two vacancies, the remaining single vacancy is not available for dissociative O_2 adsorption. It can either only be filled by a further CO molecule or remain empty. Correspondingly, when one finds an adsorbed CO_{cus} molecule only one of the two neighboring cus sites will carry an oxygen atom. The other cus site will be empty or covered with CO. This implies for the pair probability

$$P_{cus,cus}(CO, O, t) \approx \frac{\theta_{cus}(CO, t)}{2}, \quad (7)$$

i.e., at any given moment in time the probability to find a $CO_{cus}-O_{cus}$ pair is simply half the probability to find a CO_{cus} molecule at the surface at all.

Our analysis thus points at the inability of mean field to account for the correlated existence of cus vacancy pairs in the otherwise uniform adlayer as the reason for the discrepancy of PK and kMC results in the O-poisoned regime. That this is indeed correct is nicely confirmed by replacing the standard mean-field product Ansatz for the pair probabilities $P_{cus,cus}(*, *, t)$ and $P_{cus,cus}(CO, O)$, cf. Eq. (5), with the expressions in Eqs. (6) and (7), respectively. The results for a correspondingly modified PK description are also shown in Fig. 2 and reproduce the kMC data in the O-poisoned regime quantitatively.

Notwithstanding, this tailored description is not transferable to the other regimes and now fails qualitatively in the CO-poisoned regime. There, the standard mean-field PK description was perfectly valid, which can again be rationalized on the basis of the rate-determining steps. In this regime there are only three of them⁸: the adsorption and desorption of CO at cus sites, and the dissociative adsorption of O_2 at cus sites. This means that the occurrence of cus vacancy pairs is the important point in the phenomenological modeling just as before. However, on a fully CO-covered surface the main process leading to vacancy creation is CO desorption. Since this is a single-site process, vacancies are formed without any correlations and the mean-field approximation to find vacancy pairs is perfectly valid.

IV. CONCLUSIONS

In conclusion we have analyzed the previously reported failure of phenomenological microkinetic modeling to describe, in particular, the O-poisoned regime in the CO oxidation at $RuO_2(110)$. Quantitative comparison to kinetic Monte Carlo simulations shows that the error implied by the mean-field approximation amounts to several orders of magnitude in the simulated turnover frequencies, and this in a regime where the surface composition is essentially characterized by a uniform adlayer with almost 100% O coverage. This deficiency is traced back to the inability to account for the correlated existence of vacancy pairs within standard PK. Within a kinetic model without lateral interactions these pairs are not the commonly cited result of a thermodynamic segregation tendency, but instead arise out of their preferred creation by two-site O_2 desorption together with strong diffusion limitations at the oxide surface. As random single vacancies are much less prone to be refilled by O_2 adsorption, the standard mean-field expressions strongly overestimate the probability for vacancies at the surface. This leads to an overestimation for the possibility to get CO on the surface, and therewith to the observed overestimated TOFs. A modified PK approach that accounts for the predominant existence of vacancy pairs in the O-poisoned regime fixes this problem and then leads to quantitative agreement with the kMC data. However, this tailored description is not transferable and fails to reproduce the most active and CO-poisoned regime.

Next to this detailed insight into the kinetics of the specific CO oxidation model our study also provides a clear general message. Different from the widely acknowledged thermodynamic mechanism caused by lateral interactions the failure of standard PK is here the result of an incomplete adlayer randomization due to correlated vacancy creation and diffusion limitations. This kinetic mechanism leads to a breakdown of the PK approach even in the limit of an essentially uniform adlayer and in a system without significant lateral interactions. This breakdown amounts to several orders of magnitude in the simulated steady-state turnover frequencies, and is similar to our previously published findings for the transient conditions of temperature programmed desorption of a qualitative nature.⁹ While appealing in its simplicity, the PK approach proves therefore unreliable even in limiting

regimes that at first glance would appear safe in terms of its validity. In this respect, we note that this perception of safe or not safe is so far mainly derived from work on close-packed metal surfaces. On the latter, diffusion and the concomitant adlayer randomization are often fast, leaving large lateral interactions as predominant source of error for the PK approach. In contrast, on more open oxide surfaces lateral interactions tend to be smaller, while diffusion is slow. In this situation, it is more kinetic limitations such as the mechanism discussed here that challenge the prevalent mean-field modeling.

ACKNOWLEDGMENTS

Funding within the MPG Innovation Initiative Multiscale Materials Modeling of Condensed Matter and the DFG Cluster of Excellence Unifying Concepts in Catalysis is gratefully

acknowledged. We also thank Matthias Scheffler for his continuous support and inspiring discussions.

- ¹H. Lynggaard, A. Andreasen, C. Stegelmann, and P. Stoltze, *Prog. Surf. Sci.* **77**, 71 (2004).
- ²C. W. Gardiner, *Handbook of Stochastic Methods*, ed. (Springer-Verlag, Berlin, 2003).
- ³K. Reuter, in *Modeling Heterogeneous Catalytic Reactions: From the Molecular Process to the Technical System*, edited by O. Deutschmann (Wiley-VCH, Weinheim, 2011).
- ⁴I. Chorkendorff and H. Niemantsverdriet, *Concepts of Modern Catalysis and Kinetics* (Wiley-VCH, Weinheim, 2003).
- ⁵B. Temel, H. Meskine, K. Reuter, H. Metiu, and M. Scheffler, *J. Chem. Phys.* **126**, 204711 (2007).
- ⁶K. Reuter and M. Scheffler, *Phys. Rev. B* **73**, 045433 (2006).
- ⁷A. C. Hindmarsh, in *Scientific Computing*, edited by R. S. Stepleman (North-Holland, Amsterdam, 1983).
- ⁸H. Meskine, S. Matera, M. Scheffler, K. Reuter, and H. Metiu, *Surf. Sci.* **603**, 1724 (2009).
- ⁹M. Rieger, J. Rogal, and K. Reuter, *Phys. Rev. Lett.* **100**, 016105 (2008).